MC 0241.

BOX 7 FOLDER 36

Publications, 1931 - 1940

2-

Ionization and Excitation in Mercury Vapor Produced by Electron Bombardment

W. B. NOTTINGHAM

Reprinted from THE PHYSICAL REVIEW, Vol. 55, No. 2, January 15, 1939

JANUARY 15, 1939 PHYSICAL REVIEW VOLUME 55
Printed in U. S. A.

Ionization and Excitation in Mercury Vapor Produced by Electron Bombardment

W. B. NOTTINGHAM
George Eastman Research Laboratory of Physics, Massachusetts Institute of Technology, Cambridge, Massachusetts

(Received September 27, 1938)

The experimental determination of ionization and excitation in mercury vapor has been accomplished with an apparatus which permitted the evaluation of the electron energy from an accurately known magnetic field and the dimensions of the ion chamber. As a test of the apparatus the value of e/m for the electron was measured and found to be 1.758×10^7 e.m.u. A brief discussion of secondary emission and related effects is given. The ionization probability function is shown to have two important maxima, the first being at 10.8 volts and the second at 32 volts. The detailed structure between 10.4 volts and 16 volts indicates the composite character of the ionization function while the general smooth trend of the curve above 16 volts suggests that the process is relatively free from complication for high energy electrons. The study of photoelectric currents produced yielded new data on the electronic excitation function of the $2^3P_1^0$, $3^3P_1^0$, and $4^3P_1^0$ levels of the mercury atom showing that these have maxima in their probability functions at 5.6, 8.9, and 9.6 volts.

INTRODUCTION

MANY experimenters have undertaken the problem of determining the probability of ionization of mercury vapor as a function of the electron energy.[1–7] These investigators do not agree with each other except in the most superficial way since the experimental techniques differed and in no case were the methods used above criticism. The results here reported are not an exception to this rule although every effort was made to improve the experimental methods so as to be as free from criticism as possible. As the preceding paper shows, Bell obtained a confirmation of Lawrence's work but did not determine the actual yield of ions quantitatively nor did he ascertain the relative yield using an energy scale independent of uncertainties of contact potential differences. A critical examination of his experimental methods indicated the steps which should be followed in order to overcome his difficulties. The present study is thought to be the logical outgrowth of Bell's preliminary experiments.

[1] K. T. Compton and C. C. Van Voorhis, Phys. Rev. **26** 436 (1925).
[2] E. O. Lawrence, Phys. Rev. **28**, 947 (1926).
[3] A. L. Hughes and C. M. Van Atta, Phys. Rev. **36**, 214 (1930).
[4] W. M. Nielson, Phys. Rev. **37**, 87 (1931). R. D. Potter, J. Elisha Mitchell Sci. Soc. **44**, 31 (1928).
[5] P. T. Smith, Phys. Rev. **37**, 808 (1931).
[6] C. R. Haupt, Phys. Rev. **38**, 282 (1931).
[7] M. E. Bell, Thesis at Massachusetts Institute of Technology, 1937 and Phys. Rev. **55**, 201 (1939).

DESIGN AND CONSTRUCTION OF EXPERIMENTAL TUBE

General

The essential parts of the apparatus are illustrated by Fig. 1 in which a top view is shown as 1a. The cathode assembly lay in the semicircular channel formed in the face plate of the ion chamber. The electrons from the filament F were accelerated into the analyzer at slit S_1 and those of the desired energy followed circular paths to the exit slit S_2 after which they were accelerated into the ion chamber at S_3 with an increase in the mean energy by a factor of five. The radius of the electron path increased just enough for the main beam to pass out through the exit slit S_4 and into the "electron cage" EC. In the central part of the ion chamber the positive ion collector P was surrounded by two grids G_1 and G_2. The ion collector P also served as the emitter of photoelectrons when the grid potentials were arranged to exclude positive ions. The four units of this system are seen to be (1) the cathode assembly, (2) the analyzer, (3) the ion chamber with its grids and ion collector inside, and (4) the electron cage. These parts were supported mechanically by attaching the cathode assembly to the analyzer by two strong insulating members constructed as shown in Fig. 2a. The parts were all assembled by spot welding[8] tungsten to tantalum or tantalum to tantalum since no other materials were used in

[8] T. S. Gray and W. B. Nottingham, Rev. Sci. Inst. **8**, 65 (1937).

the construction. In all cases the wires were prepared for welding so carefully that practically no adjustments were needed after the welding was completed. This was necessary in order to eliminate changes in alignment during the period of severe heat treatment given to outgas the metal parts. The electron cage and its guard were mounted on the ion chamber after which the analyzer was firmly attached to the ion chamber by three insulating links. The face plates of the analyzer and the ion chamber were made from a single sheet of very flat 10-mil tantalum by sawing them exactly to size on the milling machine. The slits were also sawed with high precision so that they were in perfect alignment when the outside edges of the plates were exactly true with each other. Three heavy tantalum wires welded together to form a supporting yoke were welded to the ion chamber and the entire assembly was supported on one of the tungsten leads at the top of the tube. The tube blank with its fifteen lead-in wires was first prepared and given a twelve-hour bake under high vacuum at a temperature of 500°C in order to anneal the glass and test the seals. After this, the envelope was cracked off a few inches below the top and the assembled system mounted on a single supporting wire while the remaining electrical connections were made using 5-mil tantalum wire except for filament leads which were two 10-mil leads in parallel. A one-lead support was necessary since a glass tube of this kind undergoes a considerable deformation upon being evacuated. Eight leads were brought in through a "cluster seal" which is a circular array of wires, while the other leads came in on one triple, one double, and two single lead presses. The photographs of Fig. 3 serve to supplement this brief description of the general constructional details.

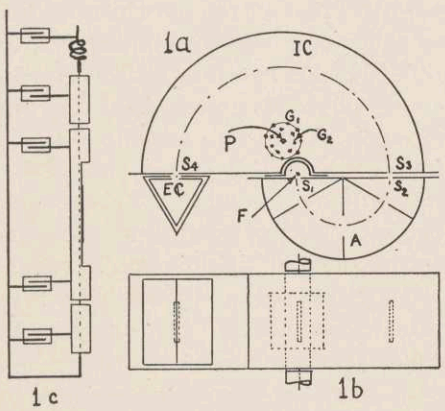

FIG. 1. Diagram of experimental tube. (a) Top view showing cathode F; analyzer A; ion chamber IC; outer and inner grids G_1 and G_2; ion collector P; and electron cage EC. (b) Front view showing location of cathode assembly and slits. (c) Side view of cathode assembly only.

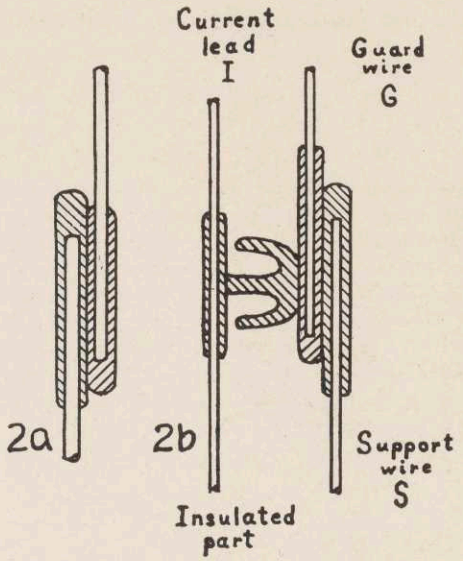

FIG. 2. Construction of insulators. (a) Insulators for mechanical support of heavy structures. (b) Insulators for extremely high insulation of the collectors.

Electron paths inside ion chamber

To a first approximation the equipotential surface halfway between the analyzer exit slit and the entrance slit of the ion chamber, was a plane parallel to the planes of the analyzer and ion chamber face plates. On each side of the median plane the equipotentials penetrated through the slits symmetrically and therefore since the electrons entered this system of equipotentials at a lower velocity than they left, the electron beam was less divergent than it would have been without this lens effect. The electrons as they entered the ion chamber formed a beam nearly homogeneous in energy and directed nearly perpendicular to the face plate of the ion chamber. When no internal field existed within the ion chamber, the electrons traveled in circles with radii proportional to the velocity. For a given magnetic field, the ion chamber voltage V_i with respect to the cathode as read on a voltmeter was adjusted to that value for which the

maximum number of electrons passed around the ion chamber and out the exit slit into the electron cage. This condition obtained when the electron densities at the two edges of the exit slit were the same. When the electron current to EC was a maximum one or two percent of the whole beam current fell on the "high energy" side of the exit slit and was collected on the inside of the ion chamber and some thirty to forty percent of the beam fell on the "low energy" side of the slit. If the voltage V_i was decreased slightly the current measured at EC decreased in spite of the additional electrons coming in on the "high energy" side of the slit because so many more electrons were intercepted on the "low energy" side of the slit. Thus by varying V_i over a small range the electron beam was made to sweep across the exit slit. If the entrance slit to the ion chamber were of infinitesimal width and all of the electrons projected into it perpendicular to the face-plate, then the diameters of all electron trajectories would lie in the plane of the face-plate and the distance from the entrance slit to the intersection of the trajectory with the face-plate would be directly proportional to the velocity. It would be a simple matter to determine the distribution in electron energy in the beam from the measurement of the current to EC as a function of the potential V_i, if these conditions were satisfied. Since the main part of the beam was more or less concentrated into a small part of the total slit width and entered the ion chamber very nearly perpendicular to the face-plate, the energy distribution in the beam was analyzed according to this scheme although it was not entirely free from objection.

In general, the gas pressure was so low that very few electrons were scattered from the beam and yet in order to make sure that the currents measured at P were due either to the arrival ions or the emission of photoelectrons, it was necessary to maintain this collector negative with respect to the filament. The large negative potential on P relative to the ion chamber repelled the electron beam as indicated by a change in the current measured at EC. By using this current as the indicator the outer grid G_1 could be made very slightly positive and the electron trajectories could be brought back to the original location, as was observed when no differences in potential were applied to the elements within the ion chamber. The ratio of the collector potential to the outer grid potential (both relative to the ion chamber) for a "neutral field" along the path of the electron beam, was 250 to one. Since this ratio was independent of the electron energy it is thought that the neutralization of the ion collector field was very nearly perfect all along the electron path in the ion chamber.

Preparation of mercury

Experience has shown that it is impossible to obtain accurate reproducibility of surface conditions over long periods of time if the experimental tube is not sealed off from the vacuum system. In order to supply the tube with a clean source of mercury vapor, a side tube containing a mercury "pellet" was attached to the main tube. This was constructed so that a "pigtail" connected to the pellet could be broken with a sliding glass hammer by turning the entire tube upside down after which, upon returning the tube to its normal position, the mercury ran out of the

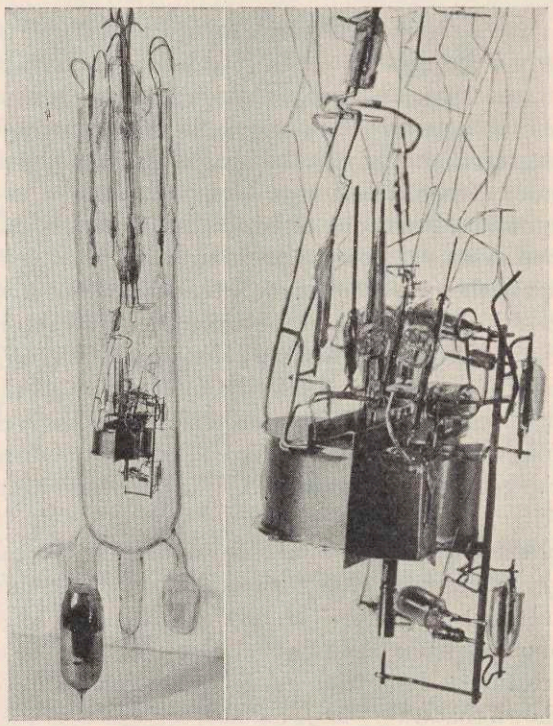

FIG. 3. Photograph of tube before attaching mercury side-arm.

opening to form a pool in the bottom of the side tube. Freshly distilled mercury was put into a still attached to a vacuum system in such a way that the mercury could be distilled out of the first still into a second one which previous to the distillation was baked for many hours at 500°C. After transferring some of the mercury from the first still to the second by slow distillation, the first one was sealed off and about two cubic centimeters of this mercury were distilled into the "pellet" which had also been thoroughly baked. During the final baking of the main tube the side tube containing the unbroken "pellet" was maintained at a temperature of about 300°C while the rest of the tube was baked at 450° to 500°C. This method of preparing the mercury was so effective that no appreciable changes were observed in the surface condition of the filament after releasing the mercury in the main tube. If a very small fraction of a monolayer of contaminating gas had formed on the filament after the release of the mercury it would have been easy to detect it.

Barium-aluminum getter

It is common practice to use a "getter" to remove the last traces of active gases such as water vapor and oxygen which even the best of diffusion pumps cannot remove to the desired degree. Eight "King Laboratories" barium-aluminum 10-mg pellets were mounted between two tantalum rings, one of which had small circular depressions punched into it to hold the pellets, while the other had small holes punched in such positions that the getter evaporated freely in the desired direction when the rings were heated to a high temperature. While the metal parts in the main tube were heated for some hours by high frequency currents a series coil also surrounded the getter ring to maintain it at a dull red heat. After the seal-off capillary was softened in preparation for the final removal of the tube, the getter was fired while the metal parts of the main tube were kept hot. The tube was sealed off after about an hour of additional high frequency heat treatment. Ionization gauge measurements have shown that a very large amount of gas is liberated when the seal-off capillary is first heated but if this is done with sufficient thoroughness no appreciable gas is given off during the actual seal-off operation.

There was some question as to the effect that getter might have in a mercury tube of this kind. Within a very short time after the release of the mercury, the getter deposit changed its appearance by taking on a brighter luster showing that a noticeable amount of mercury had condensed there. The mercury in the reservoir remained just as free from any visible contamination after it was released as before. When it was necessary to condense out the mercury to obtain additional high vacuum data which had not been obtained before the mercury "pellet" was broken, liquid air was put on the mercury side tube. This resulted in a rapid reduction in mercury pressure, as indicated both by electron scattering and by the number of ions per unit number of electrons. The residual pressure of mercury remained constant for a period of about thirty-six hours, during which measurements were made. After that time a dry-ice bath was placed on the getter side-arm and the mercury pressure soon dropped to such a low value that no mercury ions could be detected. These results are interpreted to indicate that the vapor pressure of mercury at 25°C is reduced to 0.02 percent of its normal value when covered by a film of getter.

Electrical Circuits

Filament heating circuit

The filament heating circuit was a modification of one used for the study of thermionic emission[9] and is shown schematically by Fig. 4. The 500-volt generator driven by a synchronous motor furnished power to the thyratron inverter circuit which was controlled by a 200-cycle oscillator connected to the FG-67 grids through two power amplifiers with independent gain control so as to maintain the heating period at exactly one-half cycle. A switch S_1 provided an alternative method of heating the filament from a battery for standardization. With the filament current set at the desired value, the resistance R_5 was adjusted to give a suitable current through the auxilliary filament F_2. The light from this filament fell on the FJ-114 photo-tube and the current was measured by balancing out the IR

[9] W. B. Nottingham, Phys. Rev. **49**, 78 (1936).

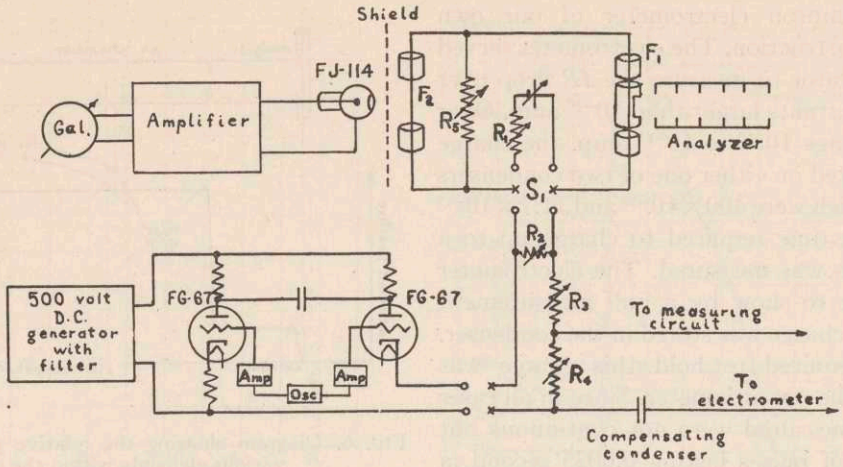

FIG. 4. Diagram of filament heating circuit and "photoelectric ammeter."

drop produced by the flow of current through a high resistance, as indicated by the FP-54 vacuum tube electrometer working in the DuBridge-Brown amplifier circuit.[10] Since it was desirable to make a large number of readings which had to be treated as "simultaneous," it was necessary to hold the filament heating conditions extremely constant and this could be done with the "photoelectric ammeter" shown.

Measuring circuits

The circuit arrangement for the application of potentials to the various elements of the tube and the measurement of currents is shown in Fig. 5. The relatvie potentials of the various elements are shown diagrammatically in Fig. 6. Before entering into the details of the main circuit mention must be made of the "compensating" condenser. Electron emission from the filament to the analyzer was cut off each heating half-cycle because the IR drop produced in resistance R_3 by the heating current made the filament 10 to 40 volts positive with respect to the analyzer depending on the value of R_3. A small capacity coupling existed between the filament heating leads and the input lead to the Compton electrometer used for measuring the small ion and photoelectric currents. By adjusting R_4 to a suitable value and applying the e.m.f. obtained there to the compensating condenser, the effect of the above-mentioned capacity coupling could be exactly neutralized.

The potentials V_1 on the focusing cylinder, V_a on the analyzer, and V_i on the ion chamber were all measured relative to the cathode with a special Leeds & Northrup type K-1 potentiometer arranged so that voltages from zero to 16.1 volts could be measured directly. For voltages higher than this the drop across a 15,000-ohm resistance in series with a 135,000-ohm resistance permitted an accurate measure of the voltage up to 160 volts. This applied particularly to the voltage V_i. Large values of the ion collector voltage $V_p{}^i$ (the superscript indicates that this is relative to the ion chamber instead of the filament) were determined by first setting the required voltage on V_i with the potential divider and then adjusting the battery on $V_p{}^i$ until the difference in potential between the ion collector P and the filament was zero. This is a necessary procedure unless more than one voltage divider is used since for accurate results the divider must be left connected to the circuit or else another 150,000-ohm resistance substituted in its place. With these methods of measurement and adequate voltage sources, all potentials were maintained and known to an accuracy of better than 0.1 percent.

The currents to the analyzer and the ion chamber were measured on carefully calibrated galvanometers and the currents to the ion collector P and the electron collector EC were measured with a small quadrant (needle radius

[10] L. A. DuBridge and H. Brown, Rev. Sci. Inst. 4, 532 (1933).

to facilitate the ready adjustment of the field current and the electrode potentials, a table was prepared for V_1, V_a, V_i, and i as a function of V_m covering the range from 5 to 100 volts. If there had been any change in contact potential difference with the time as is invariably experienced in an experimental tube continuously connected to a pumping system, it would have been impossible to use such a table and the accumulation of reliable data would have been seriously hampered.

Electron energy distribution

A typical curve which shows the observed electron current collected at EC as a function of V_i is shown in Fig. 8. These data were taken with V_a and V_1 constant and set at the optimum values as discussed above. The magnetic field current was constant and the grids and ion collector inside of the ion chamber were at the same potential as the ion chamber. The mercury was completely frozen out by the application of liquid air to the mercury side tube and dry-ice to the "getter" tube. The results obtained in this way agreed in detail with those obtained before the mercury was admitted to the tube. A logarithmic scale has been used so that one curve can present all of the data since these extend over a range of nearly 10^4 in current. In order to analyze these data we define an electron energy $V_\epsilon = V_i - 1.28$ since 1.28 volts is the "effective" contact difference in potential. With i_ϵ as the electron current received at EC, this was plotted as a function of $V_\epsilon^{\frac{1}{2}}$, as shown in Fig. 9. The curve thus obtained had two points of inflection which it is easy to show correspond to the passing of the true maximum of intensity in the electron beam across first the inner edge and then the outer edge of the exit slit as V_i (or V_ϵ) was increased. The distance in units of $V_\epsilon^{\frac{1}{2}}$ across the slit can be calculated as follows:

$$\Delta V_\epsilon^{\frac{1}{2}} = w \Big/ \frac{2\times 10^4}{H}\left(\frac{2m}{e_m}\right)^{\frac{1}{2}} = 0.038i, \qquad (4)$$

where w is the width of the exit slit in cm, H is the magnetic field, and i the current in amperes required to produce the field. In every case the observed distance between inflections agreed with Eq. (4). As V_ϵ was increased the electron beam swept across the inner edge of the exit slit adding a small increment of current to i_ϵ with each small change in V_ϵ. The slope of this curve therefore measured the distribution in electron density across the electron beam and subject to the limitations discussed above it gave the energy distribution in the beam. This simple method of determining the beam distribution applies for that range of $V_\epsilon^{\frac{1}{2}}$ which is $\Delta V_\epsilon^{\frac{1}{2}}$ wide, as given by

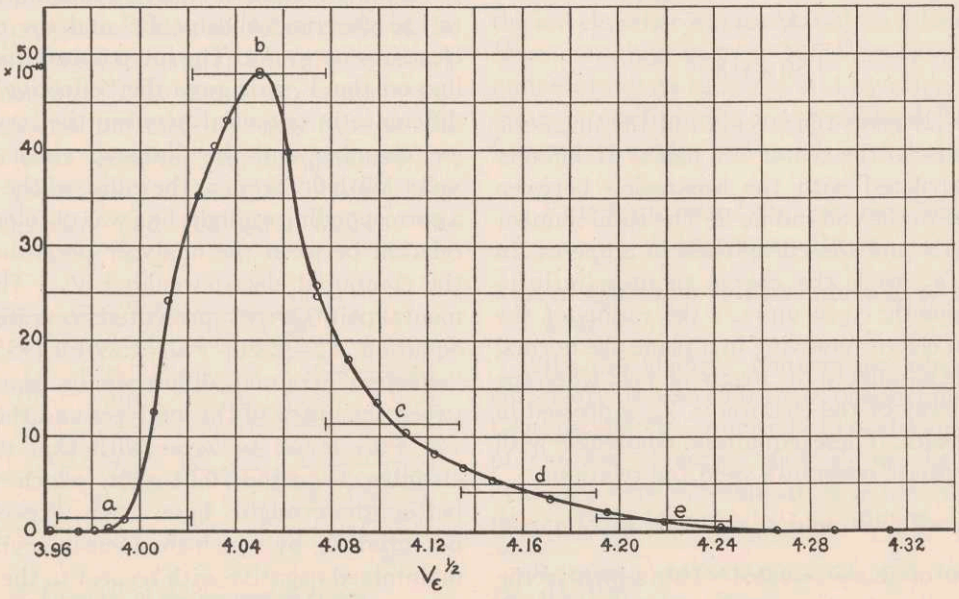

FIG. 9. Electron current collected at EC as a function of $V_\epsilon^{\frac{1}{2}}$.

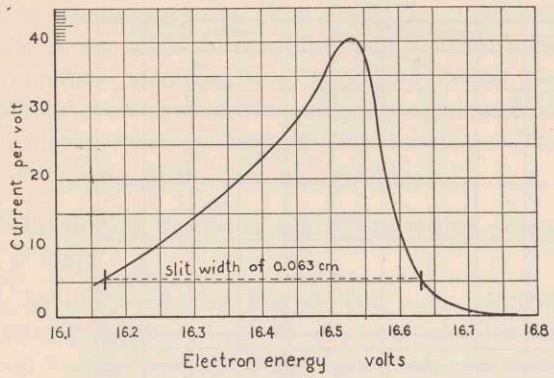

FIG. 10. Electron energy distribution subject to certain approximations.

Eq. (4), beginning at that point on the curve where the slope is appreciably different from zero. For larger values of $V_\epsilon^{\frac{1}{2}}$ than the limit of this range the slope of the curve is the difference in the ordinates of the distribution function at the two edges of the exit slit. After correcting $V_\epsilon^{\frac{1}{2}}$ by the amount $\frac{1}{2}(\Delta V_\epsilon^{\frac{1}{2}})$, the slope obtained was divided by this corrected $V_\epsilon^{\frac{1}{2}}$ and plotted against the electron energy as shown in Fig. 10. This correction is very minor but is needed to bring about a more exact correspondence to the energy distribution as related to the center of the slit instead of the inside edge.

Since it was impossible to trace the exact electron orbits from the filament through the analyzer and the ion chamber, the curve of Fig. 10 cannot be said to be a perfectly accurate representation of the energy distribution of the electrons. For reasons given above it is thought that the true energy distribution is at least as good as that shown. According to this curve nearly half of all of the electrons in the beam lie within a band only 0.15 volt wide at about 16.5 volts. If the resolving power of this apparatus is defined by this ratio, which is practically 0.01, equally careful experiments done at selected voltages from 10 to 100 volts showed that the resolving power remained very nearly constant throughout.

Determination of electron current inside ion chamber

The curve shown in Fig. 9 also served the very important function of permitting an accurate determination of the total electron current *inside* of the ion chamber. The straight lines designated "*a*," "*b*," "*c*," etc., divide the important range of observation into five segments each one slit width in extent. The intersection of the center of each of these segments with the experimental curve is a measure of the integral of all of the current in the electron beam within this range. The simple sum of these five readings which for this case was 66×10^{-10} amp., gave the total current inside of the ion chamber. Since the total current to the ion chamber including that received on the outside was 116×10^{-10} amp., the fraction delivered to the inside was 57 percent. As a function of V_m, this fraction varied from 54 percent at 10 volts to 78 percent at 100 volts. A smooth curve passed through all of the points obtained and was used in the calculation of the ionization efficiency, since for this, the number of ionic charges per unit number of electrons is needed.

Electron scattering and secondary emission effects

A characteristic feature of all of the curves giving the electron current EC as a function of

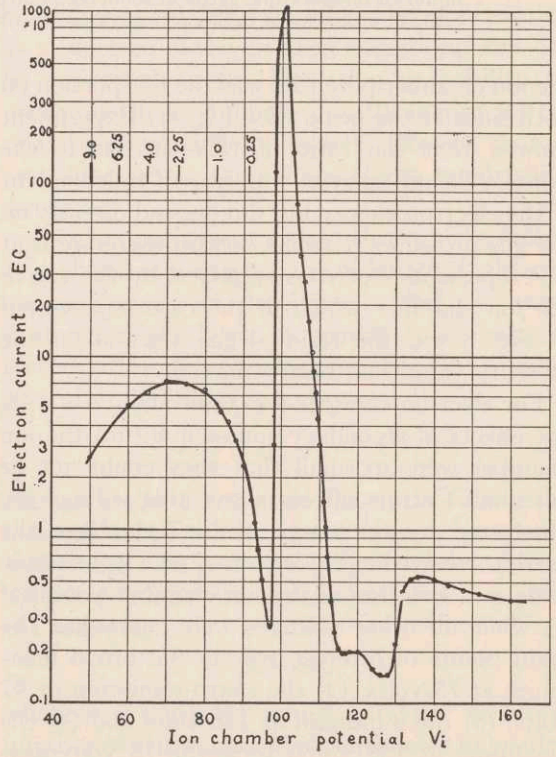

FIG. 11. Electrons collected at EC as a function of V_i showing electron scattering and secondary emission effects. Auxiliary scale for secondary electron energies.

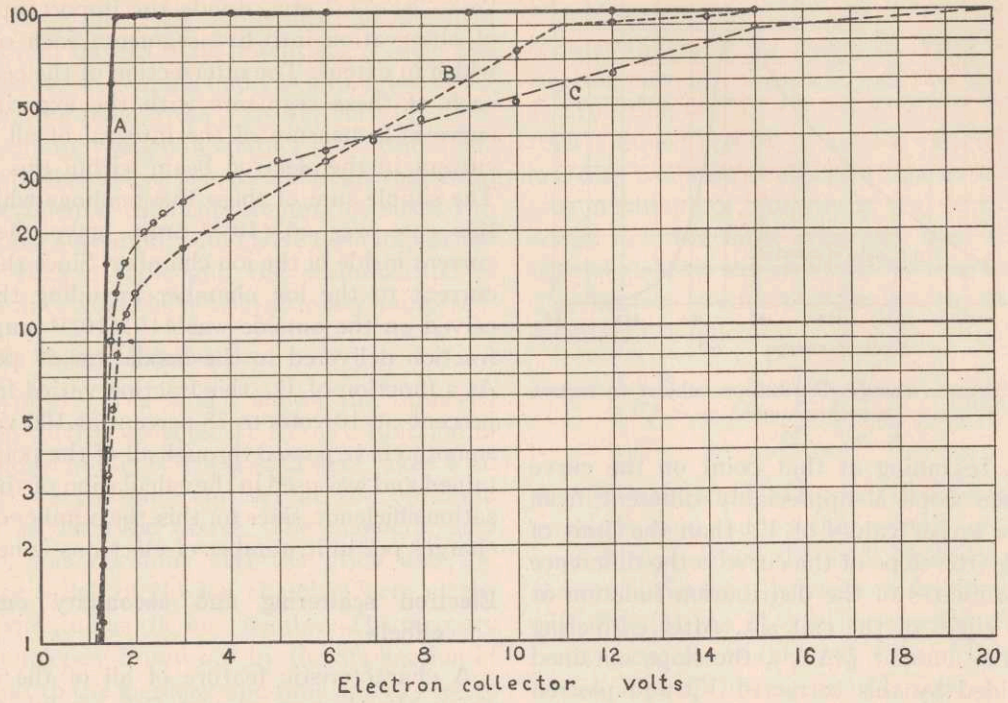

FIG. 12. Electrons collected at *EC* as a function of its potential relative to the cathode. Hg at liquid air temperature, getter at room temperature. Scattering mostly from residual mercury vapor. Scale of ordinates of each curve adjusted to 100 at maximum.

the ion chamber potential was the flat portion on both sides of the peak. (See Fig. 8.) Experiment showed that the ratio of this current to the primary beam current was nearly independent of the electron energy but did depend directly on the gas pressure. It seems certain therefore that this represents electrons scattered by the gas in the ion chamber which in the case represented in Fig. 8 was the residual gas after all of the mercury vapor had been removed.

For electron energies less than about 50 volts the effects of secondary emission within the ion chamber were so small that they could not be detected. Certain effects above this voltage are illustrated by the curve of Fig. 11. Here the current received at *EC* is plotted on a logarithmic scale as a function of the ion chamber potential V_i while all other voltages were constant. The main points of interest are (1) the broad maximum at 75 volts, (2) the sharp minimum at 97 volts, (3) the minimum at 126 volts and (4) the maximum at 135 volts. First the 75 volt maximum must have been due to the fact that a considerable number of the secondary electrons produced by the primary beam had an initial energy of two to three volts as indicated on the auxilliary scale and that these followed circular trajectories from their point of origin into the exit slit. As the beam energy increased the initial secondary electron energy which would permit its path to pass through the exit slit decreased and, since the yield to the exit slit decreased so sharply, one may interpret the 97 volt minimum as an indication that there are relatively few very low energy secondary electrons produced here. The minimum at 126 volts occurred when the main beam of electrons was projected into the right-angled corner formed at the intersection of the curved back of the ion chamber with the flat face plate. On this side of the slit very few secondary electrons found their way into the exit slit and when the beam impinged at the corner even these were absorbed more efficiently and left only the electrons scattered by the gas to give the current observed. The ratio of this current to that at the peak of the curve when compared with that of Fig. 8 illustrates the fact that the gas scattering was nearly independent

of the electron energy. The rise in the curve to a maximum at 135 volts is an indication that more secondary electrons are produced when the primary beam strikes the metal surface at grazing incidence than at perpendicular incidence. The same is true of the x-rays produced.

Collection of electrons against retarding potentials

As illustrated by Fig. 8, the main electron beam as measured at the electron collector *EC* had "wings" on both sides of the peak as a result of the scattering of the electrons by the gas molecules. By applying retarding potentials between the electron collector and the ion chamber an approximate indication of the electron energy distribution of these scattered electrons was obtained. A number of studies were made of electron energy distributions with various settings of the magnetic field and ion chamber potential. Typical of these are the three curves shown in Fig. 12 for which the magnetic field was set to permit 10.84-volt electrons to pass through the ion chamber when a V_i of 12.11 volts was applied. Curve *A* shows the current received by *EC* as a function of its potential relative to the filament when V_i was 12.11 and thus allowed the main beam to go into *EC*. It is of interest to note that no decrease in the current received was observed until the collector was less than two volts positive to the filament or until more than a ten-volt retarding potential existed between *EC* and the ion chamber. Between one and two volts the fall in current was very rapid and detailed analysis showed that this occurred about 0.3 volt sooner than it should purely from the energy standpoint. Three factors contributing to bring about this cut-off were (1) the effect of the magnetic field producing curved orbits for the slowed down electrons, (2) the bending of the electron trajectories due to the distorted electric field in the neighborhood of the slits, and (3) the possible reflection effect[9] for slow electrons.

Curves *B* and *C* were taken with values of V_i of 11.0 and 15.0 volts, respectively, and show that the energy distribution of the scattered electrons was almost Maxwellian in that it was represented by a straight line on a semi-logarithmic plot. Breaks come in these curves at 11.0 and 15.0 volts, as they should, indicating that there was no contact potential difference between the inside of the electron collector and the inside of the ion chamber.

Ionization Efficiency

Formulae for conversion of observed results to standard units

For electron energies greater than 29 volts, it is necessary to distinguish between the *efficiency* of ionization and the *probability* of ionization. The latter is defined in terms of the number of ions of a particular kind such as singly, doubly, or triply ionized atoms which are produced per electron per centimeter path while the *efficiency* of ionization is defined in terms of the total number of units of ionic charge produced per electron per centimeter path. Where ionization in mercury vapor is produced only by single collisions, there is no difference between the efficiency and the probability of ionization below 29 electron volts, but above this each doubly ionized atom contributes two charges to the efficiency function, and so on. The present study has determined only the efficiency of ionization as a function of the electron energy but this can be converted to the ionization probability by using the curves published by Bleakney[12] for the relative proportions of ions of different charges as a function of the energy of the bombarding electrons.

An electron current i_- sent through the ionization chamber along a path of length L through mercury vapor of density n atoms per cubic centimeter, produced a current i_+ of ions observed at the ion collector P (of Fig. 1a) which is given by the following formula.

$$i_+ = \alpha i_-(1 - e^{-\epsilon_i n L}). \tag{5}$$

Here α is the fraction of the total number of ions produced which found their way to the collector P and ϵ_i the ionization "cross section." This is related to the ionization efficiency E_i by the following:

$$E_i = n_0 \epsilon_i, \tag{6}$$

where $n_0 = 3.56 \times 10^{16}$ which is taken[13] to be the number of atoms per cubic centimeter in an ideal

[12] W. Bleakney, Phys. Rev. **35**, 139 (1930).
[13] R. T. Birge, Rev. Mod. Phys. **1**, 1 (1929).

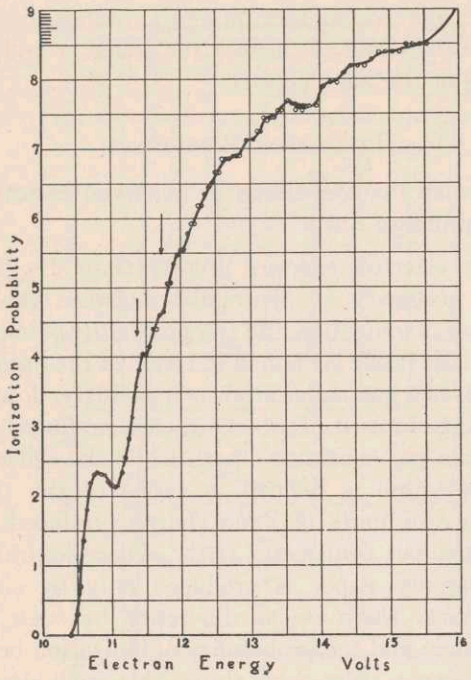

FIG. 13. Probability of ionization in mercury vapor as a function of electron energy in volts. Arrows show location of "negative energy" states.

gas at a pressure of 1.0 mm of mercury and at the temperature of 0°C or T_0°K. (If T_0 is taken at some other value than 273°K, then n_0 will be numerically different.) If T_1 is the absolute temperature of the mercury reservoir and p_1 the vapor pressure of mercury at the temperature T_1, and T is the temperature in the ionization chamber, then assuming ideal gas laws, we have the following expression for n.

$$n=n_0p_1T_0(T_1T)^{-\frac{1}{2}}. \tag{7}$$

Combining these three equations and assuming that experimental conditions are such that $\epsilon_i nL$ is very small, we obtain

$$E_i=(i_+/\alpha i_-)(T_1T)^{\frac{1}{2}}/p_1T_0L. \tag{8}$$

From the discussion so far each of these quantities is directly observable except α and this requires some further explanation. As mentioned above, the ion current was measured as a function of the electron energy with "*neutral field*" conditions along the path of ionization. Over the range for which the ionization efficiency changes rapidly with electron energy it was impossible to determine the value of α by direct measurement since the application of electric fields within the ion chamber to sweep all of the ions to the collector would have destroyed the homogeneity of the electron energies and invalidated the results. Even though the value of α depended to a certain extent on the potentials applied to the ion collector P and the outer grid G_1 to create the "neutral field" condition, it was still possible to put together a sufficient number of overlapping curves to obtain a single complete curve giving the *relative* efficiency of ionization over the entire range of observation from the ionization potential up to 100 volts. As will be shown below, there was a broad maximum in this curve as is well known from the results of previous investigators. Clearly observations made near this maximum did not depend to any great extent on the homogeneity of the electron beam and therefore in this region sweeping-out fields were applied to collect all of the ions at a collector without appreciably vitiating the results and thus allowed the determination of α.

Vapor pressure of mercury

Two sources were used for data on the vapor pressure of mercury. These were the Landolt-Börnstein tables[14] and Kelley's[15] compilation of vapor pressure data. From these two sources the following two equations were obtained:

$$\text{(Kelley)}\qquad \log_{10}p=-3283/T -0.827\log_{10}T+10.37, \tag{9}$$

$$\text{(L. and B.)}\quad \log_{10}p=-3342.26/T -0.847\log_{10}T+10.5724. \tag{10}$$

The range of application of the latter formula is given as $-10°$ to $+200$°C. The two formulae above agree very well over the range needed for the present study and can be represented to the required accuracy by the equation

$$\log_{10}p=8.12-3220/T, \tag{11}$$

or

$$p=132\times10^6e^{-7415/T}. \tag{12}$$

In all of the above equations the pressure is given

[14] M. Knudsen, Ann. d. Phys. 29, 179 (1909); Landolt-Börnstein, Vol. II (1923), p. 1334.
[15] K. K. Kelley, Bureau of Mines Bulletin 383.

in millimeters of mercury and the temperature is in °K.

Ionization near the ionization potential

The final results obtained for the ionization probability in the immediate neighborhood of the ionization potential are presented in Figs. 13 and 14. The general similarity between the curve of Fig. 13 and that obtained by Lawrence[2] is at once obvious. In Fig. 14 the ionization probability has been plotted on a logarithmic scale in order to make available the data obtained within the first few tenths of a volt of the ionization potential. The circles shown give the results as observed without making corrections for the slit width and a small photoelectric current of electrons released from the ion collector by the radiation in the ion chamber. Since the details as to the distribution of electron energies could not be known exactly, it was impossible to apply a rigorous method for reducing the observed results to an accurate ionization probability curve. Approximate methods were used with the result that the solid line shown is thought to be as accurate a representation of the actual probability curve as can be drawn.

The maximum observed at 10.8 volts and the minimum at 11.05 volts are in some ways the most interesting details of the curve. It is quite possible that the cathode fall in a mercury arc discharge is stabilized to a considerable extent because of the fact that 10.8-volt electrons have a higher probability of producing ions than other electrons with energies up to 11.15 volts. The other structural features shown in Fig. 13, are no doubt of less practical significance but may be important to the detailed understanding of the collision process in mercury vapor.

It hardly seems necessary to attribute these irregularities to "ultra-ionization" potentials as is usually done.[2–6] The interpretation which seems most natural is closely related to the proposals made by von Hippel.[16] As will be shown below, the excitation of the $2^3P_1^0$ state of the mercury atom from the 1^1S_0 state, by electron bombardment has zero probability at 4.87 volts (the minimum energy for excitation) but at 5.6 volts the electron has its maximum probability of producing this transition. Although this experiment can not be said to be absolutely conclusive for reasons which will be given, the indications were that no such clear maximum exists for the transition to the 2^1P_1 state. The possibility that the excitation function for intercombination transitions generally has a maximum within a few tenths of a volt of the minimum energy required for excitation and that terms within the singlet system may not have this maximum so near to the minimum excitation potential has been recognized for some time. Since the series limits of both the triplet series and the singlet series are at 10.38 volts it seems reasonable to suppose that the probability of ionization would have a twofold character and that the peak at 10.8 volts might be ionization according to the mode of the principal triplet series while the general background and broad maximum at about 32 volts is to be associated with ionization without change in spin momentum which characterizes the singlet system. Other details, which may be seen between 11.5 and

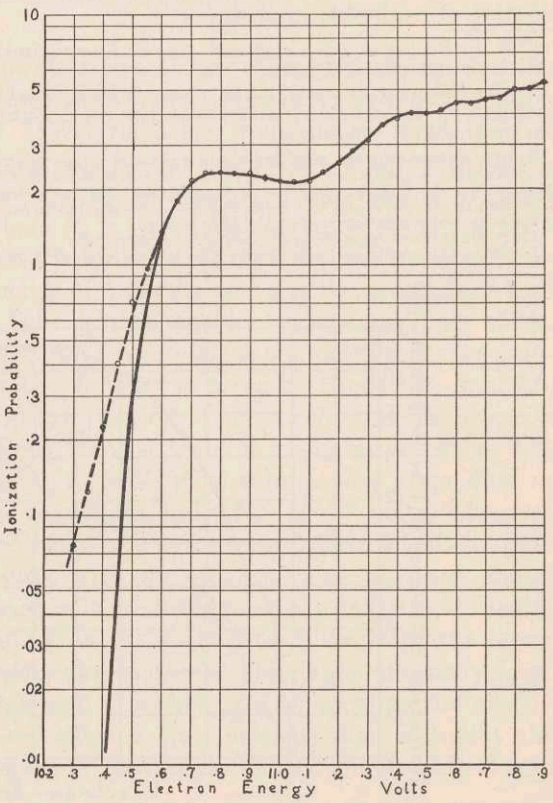

FIG. 14. Probability of ionization showing details within first volt from ionization potential.

[16] A. von Hippel, Ann. d. Physik **87**, 1035 (1928).

15.5 volts, may be due to the influence of the "negative energy" states which involve the initial absorption of energy by both of the valence electrons with the ultimate expulsion of one of these electrons with considerable kinetic energy and the return of the atom to the unexcited ionized state. The location of two of the known "negative energy" states[17] are indicated on Fig. 13 by arrows. The fact that "kinks" occur near these points may be without significance since the probability curve for a particular mode of excitation cannot be expected to have a high value when the electron energy barely exceeds the minimum required for its excitation. In some ways it seems that the more complicated the process of excitation is the nearer the maximum of the probability curve comes to the minimum energy value. Above 15.5 volts no detailed structure could be clearly demonstrated. This suggests that within the first two or three volts of the ionization potential the probability curve is dominated by the superposition of a number of modes of ionization while above 15.5 volts these become of negligible importance.[18]

[17] R. F. Bacher and S. Goudsmit, *Atomic Energy States*, (McGraw-Hill 1932), p. 227.

[18] The following analysis of the energy states expected as based on theoretical considerations has been worked out by Dr. W. E. Albertson.

Since it appears that the most prominent excitation peaks are due to intersystem combinations of the type $^1S_0 - {}^3P_1^0$ it is of interest to speculate on the probable positions of those peaks which arise from excitation to other $^3P_1^0$ and $^3D_1^0$ levels theoretically expected to occur in mercury, but which have not as yet been found.

There are three electron configurations of interest, namely:

$5d^9 6s^2 6p$—this configuration will give rise to the levels $^3P_1^0$, $^1P_1^0$, and $^3D_1^0$, all of which have J values of one. Consideration of the relative bindings of the $5d$ and $6s$ electrons indicates that the terms of this configuration occupy the region 8.1 to 11.0 volts above the ground state. $^3P_1$ and $^3D_1$ will probably be below the I.P. (10.38 volts), whereas $^1P_1$ may be close to, but above the I.P.

$5d^{10} 6p 7s$ and $5d^{10} 6p 6d$—the former will give rise to the combining levels $^3P_1^0$ and $^1P_1^0$, the latter to $^3P_1^0$, $^1P_1^0$ and $^3D_1^0$. Since the excitation to these states involves a two-electron jump from $5d^{10} 6s^2$, it is quite possible that the resulting peaks will be comparatively insignificant.

A rough evaluation of the energies of these configurations may be made by considering the difference in energies between the $6s$ electron and the $7s$ and $6d$ electrons and adding those energies to that of the $5d^{10} 6p 6s$ configuration.

The difference in energy between $6s^2$ and $6s7s$ is 7.8 volts, hence the excitation potential of $5d^{10} 6p 7s$ will be, to a first approximation, 4.6 plus 7.8 or 12.4 volts. The levels from this configuration should spread over a region of about two volts, hence the excitation potentials should be near 12.4 volts and on up to 14.4 volts.

In like manner it can be estimated that the excitation potentials for levels from $5d^{10} 6p 6d$ should be near 13.4 volts and on up to 15.4 volts.

While these estimates are not necessarily accurate to within a volt, they do fall in the range necessary to afford a plausible explanation of several of the minor excitation peaks between 12.5 and 14.5 volts.

(For notation see Chap. XII of H. E. White, *Introduction to Atomic Spectra*, (McGraw-Hill, 1934).)

Ionization by high energy electrons

When mercury vapor is bombarded by electrons with energies exceeding 29 volts, both singly and doubly charged ions are produced with the result that the *efficiency* of ionization is observed instead of the *probability*. The solid curve of Fig. 15 shows the result obtained. Bleakney[12] observed in a mass spectrograph the relative proportions of singly ionized and doubly ionized atoms as a function of the electron energy. His curves were used to reduce the observed efficiency curve to the probability curve, as shown by the dashed line of Fig. 15.

The dotted curves of this figure present the results obtained by Smith[5] and by Compton and

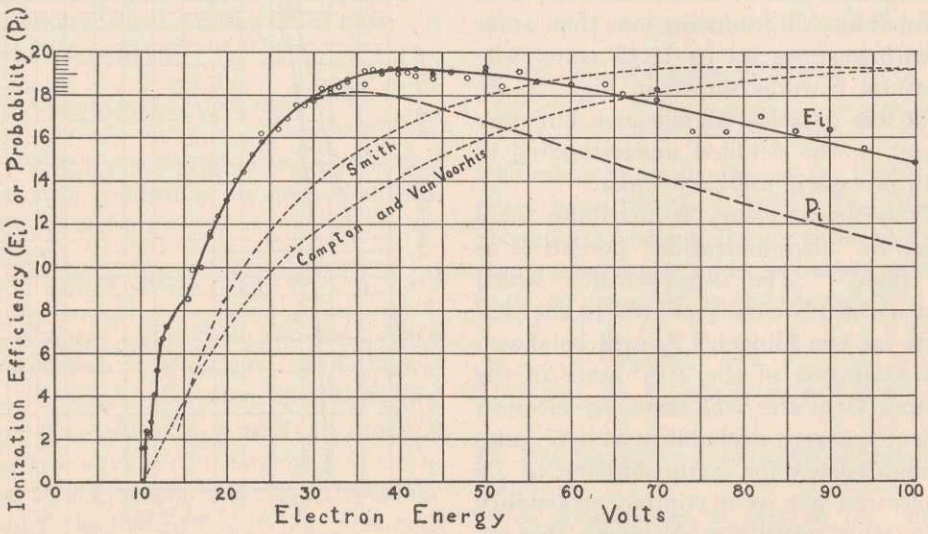

FIG. 15. Efficiency of ionization as a function of electron energy. Dashed curve P_i is probability of ionization with the loss of only one electron. Correction depending on Bleakney's curves.[12]

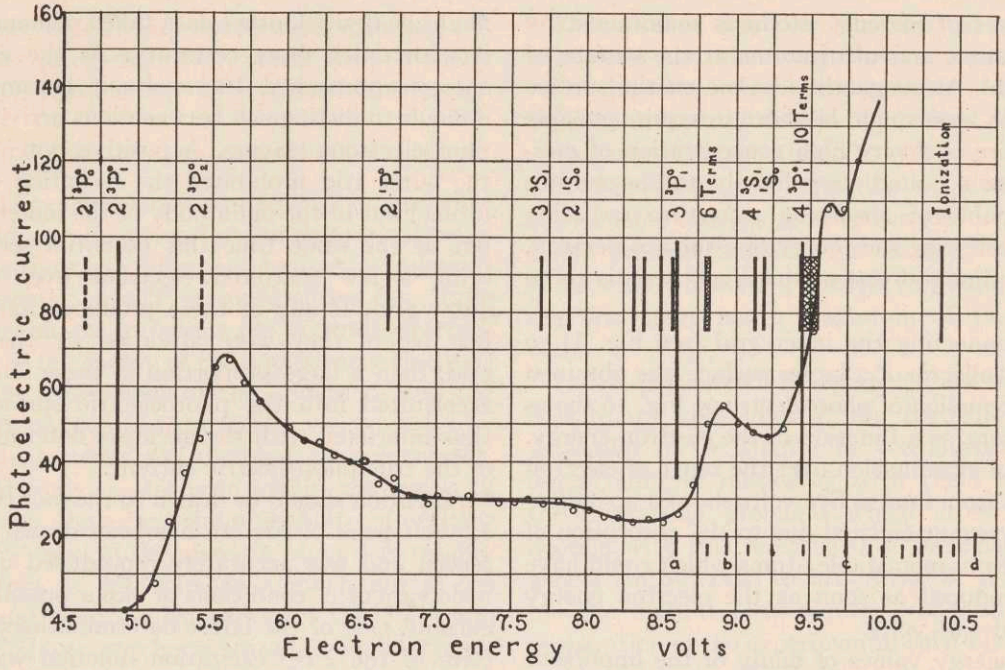

FIG. 16. Photoelectric current from inner grid and electrode P as a function of electron energy. Energy levels of mercury shown above and Smith's[5] critical potentials displaced downward 1.8 volts, shown at lower right. Onset at "a," larger deviations at "b" and "c," hump between "d" and "e."

Van Voorhis.[1] Comparison of these different efficiency curves shows that reasonable agreement exists but the differences greatly exceed the estimated errors in each case. Although certain difficulties experienced by the previous investigators can be pointed out, it cannot be said that the differences are explained in that way. In the present case every test that could be devised to test the validity of the final results was used. Under all circumstances the fact that the ion current was accurately proportional to the electron current indicated that ionization by multiple collisions could be neglected. The ion current was observed to be directly proportional to the mercury density in the ion chamber. This served to show that very few electrons produced ionization at more than one collision. The data for the probability curves shown were taken with the mercury reservoir at 0°C.

EXCITATION OF OPTICAL LEVELS

Excitation of $\lambda = 2537$A radiation

Because of the small area of the ion collector P only one quantum in 1500 was intercepted by this electrode. It was thought therefore that the photoelectric current produced by the absorption of 2537A radiation would be so weak that it could not be detected. This was found not to be the case for experiment showed that $\beta P_e = 0.4$ where P_e is the probability of exciting the $2^3P_1^0$ state from the 1^1S_0 state by electrons with an energy of 5.6 volts and β is the probability that a light quantum which strikes any part of the collector P will emit a photoelectron. The collision probability as given by Brode[19] is about 120 and the fraction of these collisions which excite atoms to this state is probably between 0.01 and 0.1. Seiler's[20] determination gives 0.04 at his maximum and 0.025 at 5.7 volts. This sets the range of β to be from 0.33 to 0.033. In other words, with the smaller value of β one photoelectron is produced for every thirty light quanta falling on the surface of P, or, with the larger value, one in three. This is an unusually large yield and probably calls for some special mechanism which is more efficient than is usually the case. For example, it might be possible that a

[19] R. B. Brode, Proc. Roy. Soc. **A125**, 134 (1929).
[20] R. Seiler, Zeits. f. Physik **83**, 789 (1933).

monolayer of mercury atoms is maintained by the constant arrival of atoms at the surface of the metal. Although the lifetime on the surface of a given atom might be short, it is quite possible that there is a very high concentration of mercury atoms bound very loosely to the surface and capable of absorbing resonance radiation and transferring the energy to a surface electron. An experimental test of this hypothesis is to be made.

By connecting the inner grid (see Fig. 1) to the ion collector P a larger surface was obtained for the emission of photoelectrons. Fig. 16 shows the current as a function of the electron energy. A careful examination over the range of electron energies from four to five volts showed no indication of current emitted due to the absorption of energy from metastable atoms which could have been produced as soon as the electron energy exceeded 4.65 volts.

The energy values of many of the important terms of the mercury spectrum are shown on Fig. 16. A comparison between the observed current and the indicated energy levels shows that the 5.6-volt peak with its onset at 4.9 volts must be associated with the $2^3P_1^0$ transition. There may be two explanations for the fact that there was no important variation in the photoelectric current as the electron energy exceeded that required to excite the $2^1P_1^0$ level. These are, first, the surface might not have been as sensitive photoelectrically to the $\lambda = 1849$A radiation as it was to the 2537A radiation for which it seemed to be abnormally sensitive, and secondly, it is possible that the probability function associated with this transition may start rising very slowly and reach important values at ten or more volts. The sharp rise in photoelectric current beginning at 8.6 volts and reaching a maximum at 8.9 volts seems to be definitely related to the $3^3P_1^0$ term located at 8.60 volts. The next peak located at 9.62 volts is probably associated with the excitation of the $4^3P_1^0$ level which requires a minimum energy of 9.44 volts. The onset in this case is less distinct because of the rapid rise in general background of photoelectric current which becomes so important for energies greater than 9.0 volts. Although the set of data presented in Fig. 16 does not establish the existence of the 9.6 volt peak as convincingly as might be desired, other data taken demonstrated it with much more certainty. As the electron energy approached 10.4 volts it became very difficult to distinguish between ions arriving and photoelectrons leaving. A positive potential on the outer grid prohibited the reception of ions formed out in the main body of the ion chamber but at the same time this potential served to bring a few scattered electrons over to the outer grid. If any of these produced ionization just before they were absorbed by the outer grid, then a large proportion of these ions were accelerated into the photoelectric surface and thus interfered with the accurate determination of the true photoelectric current.

Attention should be drawn to the fact that the 5.6-volt peak of Fig. 16 has been drawn as observed and was accurately reproduced under a wide variety of conditions of vapor pressure and current. One of the latest determinations of the form of the $2^3P_1^0$ excitation function was that of Seiler[20] whose observations were much more indirect in character and led him to conclude that the maximum of the probability function occurred at 6.9 volts. A redetermination of this function using experimental techniques so as to measure the absolute values of the probability function, would no doubt be of great value.

A critical examination of Smith's[5] experimental results leads to the interpretation that some of his "ultra-ionization" potentials were due to photoelectric effects. In his Fig. 7 there is a very noticeable "hump" in the curve near 12.6 volts according to his scale. If it is assumed that this is the 10.8 volt maximum of Fig. 13 then a displacement of his set of critical potentials by 1.8 volts would be demanded. With the intervals maintained as published by Smith, these critical potentials have been recorded, as shown in Fig. 16. It is obvious at once that this displacement brings his first value (a) to 8.6 volts, which marks the beginning of the big rise in the photoelectric current. Critical potentials at (b) and (c) corresponded to larger deviations from a smooth curve than some of the others and might be related to the maxima at 8.9 and 9.6 volts. The "hump" mentioned above lies between (d) and (e). There are many term levels between 9 and 11 volts which are not shown in the figure and since some of these no doubt have excitation

functions which rise rapidly and then fall off, it seems altogether likely that Smith's many critical potentials may be explained in this way.

Summary and Conclusions

1. It has been demonstrated that it is possible to build an apparatus for the determination of the electronic excitation and ionization functions of mercury, which is sufficiently free from spurious effects to permit the accurate determination of the energy of the bombarding electrons from the dimensions of the apparatus and the strength of the magnetic field.

2. Measurements of the photoelectric current, emitted from an electrode within the region of excitation, show that the probability of exciting the $2^3P_1^0$ level of the mercury atom rises rapidly from zero at 4.9 volts to a maximum at 5.6 volts and that the excitation of the $3^3P_1^0$ and the $4^3P_1^0$ levels are characterized by similar curves with maxima at 8.9 and 9.6 volts, respectively.

3. Ionization has been observed to set in at 10.4 volts and rise to a distinct maximum at 10.8 volts followed by a minimum at 11.05 volts. Definite structural details of a minor character were observed up to about 16 volts.

4. The *efficiency* of ionization has a maximum of 19.2 ionic charges per electron per cm path at 1 mm pressure and 0°C for an electron energy of 42 volts while the *probability* of ionization to the first stage has a maximum of 18.2 at 32 volts.

It is a pleasure to acknowledge my indebtedness to my colleagues at the Institute and in particular to Dr. Arthur R. von Hippel for the opportunity of discussing with them many of the interesting problems which arose in connection with this research. For technical assistance I am indebted to Mr. Allyn B. White and for the skillful glass-blowing required in the preparation of the experimental tube I owe much to Mr. Lawrence W. Ryan.

LANCASTER PRESS, INC., LANCASTER, PA.